ORIGINAL PAPER

LiFePO4/C composites from carbothermal reduction method

H. Liu · P. Zhang · G. C. Li · Q. Wu · Y. P. Wu

Abstract Using the cheap raw materials lithium carbonate, iron phosphate, and carbon, LiFePO4/C composite can be obtained from the carbothermal reduction method. X-ray diffraction (XRD) and scanning electronic microscope (SEM) observations were used to investigate the structure and morphology of LiFePO4/C. The LiFePO4 particles were coated by smaller carbon particles. LiFePO4/C obtained at 750 °C presents good electrochemical performance with an initial discharge capacity of 133 mAh/g, capacity retention of 128 mAh/g after 20 cycles, and a diffusion coefficient of lithium ions in the LiFePO4/C of 8.80×10^{-13} cm^2/s, which is just a little lower than that of LiFePO4/C obtained from the solid-state reaction (9.20×10^{-13} cm^2/s) by using FeC_2O_4 as a precursor.

Keywords LiFePO4 · Carbothermal reduction · Lithium ion battery

Introduction

Since the first report of the LiFePO4 in 1997 [1, 2], it has been widely investigated as a promising cathode material to substitute $LiCoO_2$. The LiFePO4 has high theoretic capacity as 170 mAh/g [2], has high charge/discharge potential

---

H. Liu · P. Zhang · G. C. Li · Y. P. Wu
Department of Chemistry and Shanghai Key Laboratory of Molecular Catalysis and Innovative Materials, Fudan University, Shanghai 200433, China

Q. Wu · Y. P. Wu (✉)
L&F Co. Ltd, 703-13 Hosan-Dong Dalsu-Gu,
Daegu 704-220, South Korea
e-mail: wuyp@fudan.edu.cn

(3.4 V vs. Li^+/Li) [3], has rich source, and has environmental benignancy [4]. The main disadvantage of this material is the poor conductivity [1, 4], which causes rapid capacity loss at high rate. Conventional approaches to overcome the disadvantage are conductive agent coating [5–7] and heteroatom doping [8–10].

There are a lot of methods to synthesize purified LiFePO4, for instance, solid-state reaction [5, 11], hydrothermal method [12, 13], sol–gel synthesis [14–16], and other unusual approaches such as spray solution technology [17] and template technology [18]. Generally speaking, most synthesis methods are basically using the Fe^{2+} source. For the economic consideration, using the Fe^{3+} source to synthesize can decrease the cost. Crystalline LiFePO4 can be synthesized by heating amorphous LiFePO4, which is reduced from amorphous $FePO_4$ by the reductive agent LiI [19, 20]. This method is too inconvenient to obtain the LiFePO4. Carbothermal reduction method is a simple and cheap way to obtain the LiFePO4 from the Fe^{3+} source. High-capacity carbon-coated and magnesium-doped LiFePO4 can be synthesized using LiH_2PO_4, Fe_2O_3, and carbon as raw materials by carbothermal reduction (CTR) method [21]. But here, the LiH_2PO_4 is also an expensive reagent. LiFePO4 can be also obtained by aqueous precipitation and carbothermal reduction from $FeSO_4$ $7H_2O$ [22], but this route seems too fussy. Pure LiFePO4 without traces of the Fe (III) phase such as Fe_2P and/or Fe_2O_3 can be obtained from the starting materials $FePO_4(H_2O)_2$, Li_2CO_3 in isopropyl ethanol [23]. High-density spherical $Li_{0.97}Cr_{0.01}FePO_4$/C cathode material can be synthesized using the mixture of spherical hexagonal $FePO_4$, Li_2CO_3, $Cr(NO_3)_3$ and sucrose [24]. But the latter two ways are not real carbothermal reduction methods because the Fe^{3+} was reduced not only by the reductive carbon, but also by reductive atmosphere or hydrogen from the decomposed organic compound.

In this paper, we synthesized the LiFePO₄/C from very cheap raw materials FePO₄ 4H₂O, Li₂CO₃ and carbon by the one-step CTR method. Here, only the reductive carbon, but not the cooperation of carbon and hydrogen, reduces the Fe^{3+} in this method.

Experimental

LiFePO₄/C composite was synthesized from the carbothermal reduction method. The starting materials Li_2CO_3, FePO₄ • 4H₂O, and acetylene black (AB) were mixed at the molar rate of 1:2:4. The mixtures were milled in a planet mixer (QM-BP) for 24 h. After milling, the mixtures were calcined in a tube furnace with argon flow at 700, 750, and 800 °C for 15 h as in the following equation:

$$Li_2CO_3 + 2FePO_4 + 2C = 2LiFePO_4 + 3CO \uparrow \qquad (1)$$

The carbon in the raw materials acts as reductive agent. The outcome LiFePO₄ and excess AB can form the LiFePO₄/C composite.

The electrodes were prepared by mixing 90 wt% active material, 5 wt% acetylene black as conductive agent, and 5 wt% polyvinylidene fluoride (PVDF) binder in N-methylpyrrolidone (NMP) solvent to form a homogeneous slurry. Then, the mixtures were coated on an aluminum foil and punched to disks. After drying under ambient condition, the disks were further dried in vacuum oven at 120 °C for 12 h. Finally, coin-type cells were assembled in a glove box, using lithium foil as the counter and reference electrode, Celgard 2400 as the separator, and LIB315 (Guotai Huarong Chemical Plant) as the electrolyte.

Powder samples were identified using a powder X-ray diffractometer (D8, Bruker) with monochromatized CuK_α radiation. The surface morphology was observed with scanning electronic microscope (SEM, Philips XL 300). Both electrochemical impedance spectroscopy (EIS, EG, and G5210) and cyclic voltammetry (CV, CHI600) were evaluated in a two-electrode cell at room temperature. The CV curve was carried out at the range of 2.0–4.5 V. In EIS measurement, the frequency range was between 100 kHz and 10 mHz with the excitation voltage 10 mV applied to the cells.

Results and discussion

The X-ray diffraction (XRD) patterns of LiFePO₄/C obtained from CTR technology at 700, 750, and 800 °C are shown in Fig. 1, which are mainly consistent with the olivine structure and indexed to the orthorhombic P_{nmb}
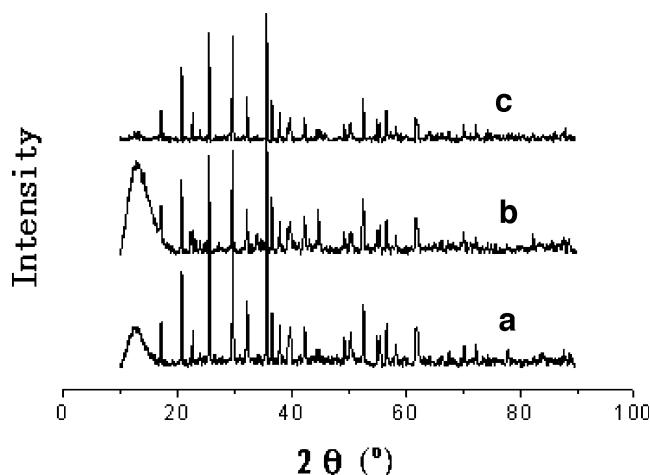

Fig. 1 X-ray diffraction patterns of the LiFePO₄/C composites from CTR method at different temperatures: **a** 700 °C, **b** 750 °C, and **c** 800 °C

space group. Some minor peaks around the baseline are due to the impurities, which can be mostly attributed to $Li_3Fe_2(PO_4)_3$ [22, 25, 26], which might effect the electrochemical performance of the as-prepared samples.

The morphologies from SEM observations of LiFePO₄/C at different temperatures are shown in Fig. 2. It is clear that all LiFePO₄ particles from different reaction temperatures are coated with small AB particles, which can favor the increase of electronic conductivity of the as-prepared samples. From thermogravimetric analysis, it was found that the amount of AB in the LiFePO₄/C composite is approximate to 10% in LiFePO₄/C composite, which is higher than the calculated carbon residue (7.1%) based on the original addition amount. The sizes of the particles are ranging from 1 to 3 μm. The crystalline particle grows with the increase of the temperature. When the reaction temperature reaches 800 °C, partial particles grow to bigger bulks. It is known that the bigger particle of LiFePO₄ is not good for the diffusion of lithium ions due to the longer pathway for migration than the smaller particles.

Figure 3 shows the initial voltage profiles of LiFePO₄/C composite from CTR method. The charge/discharge curves with flat plateaus correspond to the lithium de-intercalation and intercalation reactions. During the first cycle, the LiFePO₄/C electrode in 700, 750, and 800 °C show the charge/discharge capacity of 138/110, 150/133, and 122/86 mAh/g, respectively, which demonstrate that the sample obtained in 750 °C has the highest initial capacity. However, the reversible capacity is lower than the theoretic value of 170 mAh/g.

The cycling performances of the prepared LiFePO₄/C composites are shown in Fig. 4. The discharge capacities are fluctuant during the cycles, which is mainly due to the impurity in the samples. After 20 cycles, the discharge
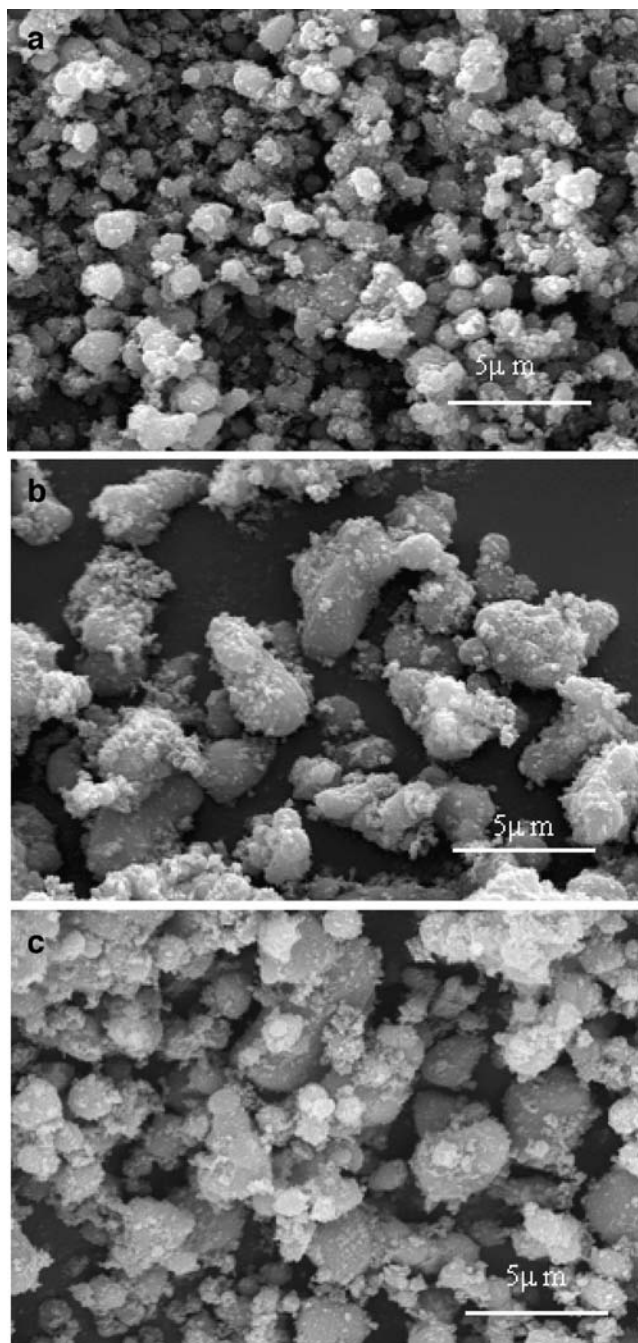
Fig. 2 SEM micrographs of the LiFePO$_4$/C composites from CTR method at different temperatures: **a** 700 °C, **b** 750 °C, and **c** 800 °C
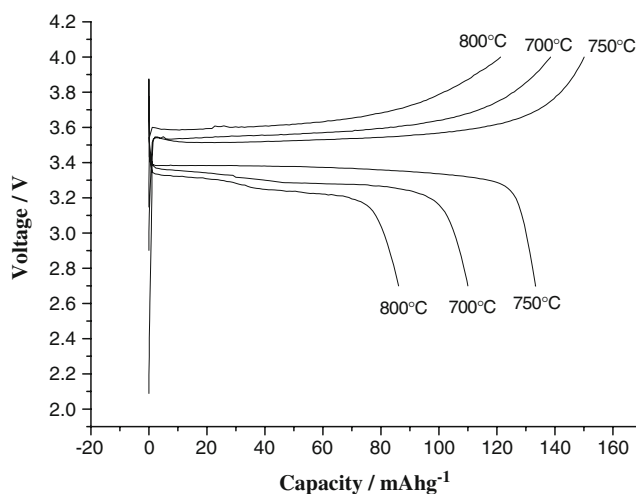

Fig. 3 Charge and discharge curves at the 0.1C in the first cycle of the prepared LiFePO$_4$/C composites

intercalation/de-intercalation process. The symmetrical shape of the anodic/cathodic peaks indicates that the electrochemical intercalation/de-intercalation of lithium ions in the electrode material is highly reversible.

The Nyquist plot of the LiFePO$_4$/C electrodes synthesized at 750 °C is shown in Fig. 6, which was measured in the fully discharged state. The profiles exhibit a semicircle in the high frequency region and a straight line in the low frequency region. The depressed semicircle in the high frequency region is attributed to the charge transfer process [27]. The numerical value of the diameter of the semicircle on the Z_{re} axis is approximate to the charge transfer resistance (R_{ct}). At low frequency region, the straight beeline represents a typical Warburg behavior, which is relative to the diffusion of lithium ions in the active cathode material. The diffusion coefficient of lithium ions could be
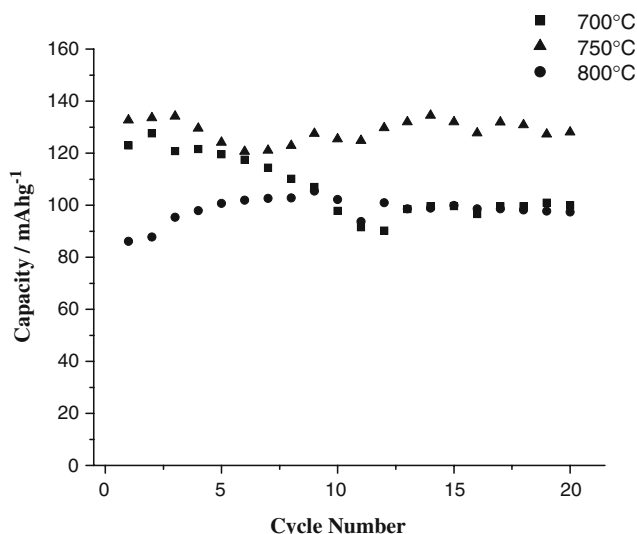
capacities of electrode materials obtained in different temperatures are 100, 128, and 97 mAh/g. The LiFePO$_4$/C composite obtained at 750 °C from the CTR method, with the moderate particles size, exhibits the best capacity retention of 96%.

The cyclic voltammetric profile of the LiFePO$_4$/C composite obtained at 750 °C is shown in Fig. 5. The well-defined redox doublet located at 3.66/2.78 V represents the inter-transformation of Fe^{2+} and Fe^{3+} during

Fig. 4 Cycling performance of the prepared LiFePO$_4$/C composites at the current density of 0.1 C rate in voltage range of 2.7–4.0 V
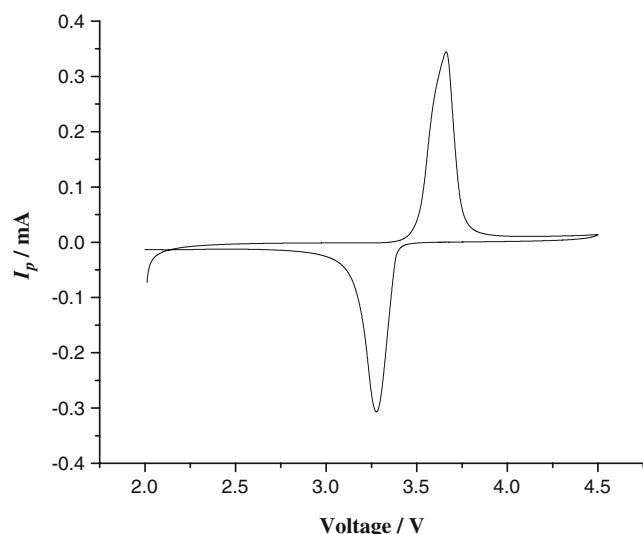
Fig. 5 The cyclic voltammogram of the LiFePO$_4$/C synthesized at 750 °C for 15 h by CTR method

calculated from the low frequency spots according to the following equation [28]:

$$D = R^2 T^2 / 2A^2 n^4 F^4 C^2 \sigma^2 \tag{2}$$

where R is the gas constant, T is the absolute temperature, A is the surface area of the cathode, n is the number of electrons per molecule during oxidization, F is the Faraday constant, C is the lithium ion concentration in electrode material, and σ is the Warburg factor which is relative with Z_{re}.

$$Z_{re} = R_D + R_L + \sigma \omega^{-1/2} \tag{3}$$

The relationship between Z_{re} and reciprocal square root of frequency ($\omega^{-1/2}$) in the low frequency region is shown
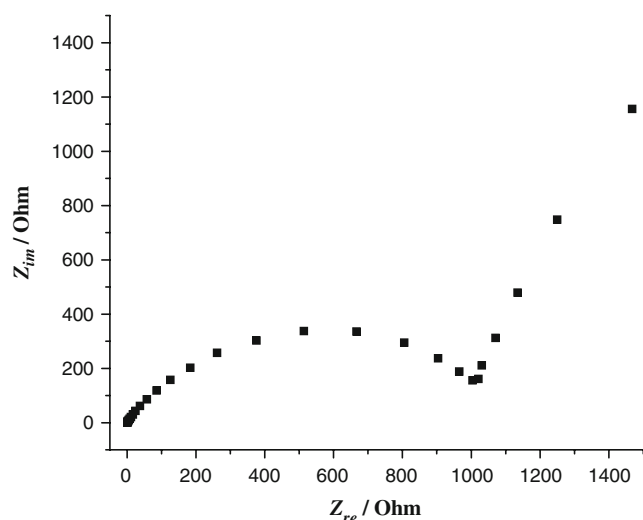

Fig. 6 The Nyquist plot of the LiFePO$_4$/C composite electrode synthesized at 750 °C in the frequency range between 100 kHz and 10 mHz
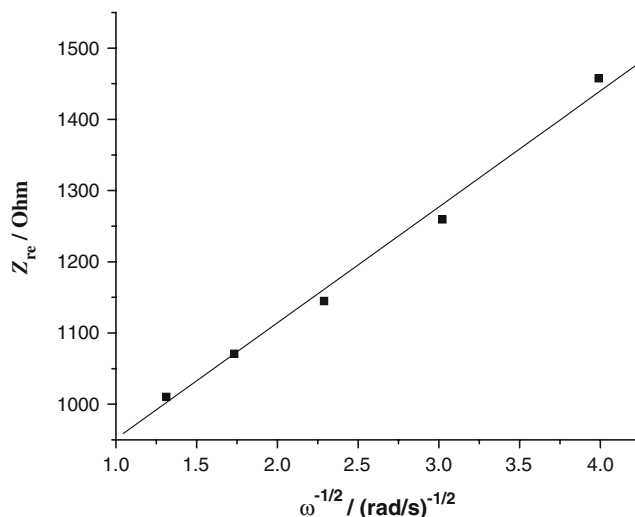

Fig. 7 The relationship between Z_{re} and $\omega^{-1/2}$ at low frequency for the LiFePO$_4$/C composite electrode synthesized at 750 °C

in Fig. 7. The diffusion coefficient of lithium ions in the LiFePO$_4$/C was calculated to be 8.80×10^{-13} cm^2/s, which is just a little lower than that of LiFePO$_4$/C obtained from the solid-state reaction (9.20×10^{-13} cm^2/s) by using FeC$_2$O$_4$ as the precursor [5], also suggesting the effectiveness of this method. For the cathode materials, the crystal structure plays an important role to lithium ion intercalation/de-intercalation. In the case of LiFePO$_4$/C composite obtained from our CTR method, the impure Li$_3$Fe$_2$(PO$_4$)$_3$ perhaps baffles the diffusion of lithium ions in the bulk LiFePO$_4$/C composite.

Controlling the amount of impurities in LiFePO$_4$/C composite is the possible problem to overcome for this CTR method. Given the complete elimination of impurities, the crystal structure and the diffusion of lithium ions of LiFePO$_4$/C composite would be much improved. Further studies with this CTR technology is necessary, as it is very promising and of special significance for the industrialization of the LiFePO$_4$ material.

Conclusion

LiFePO$_4$/C composite has been successfully obtained from the one-step CTR in different temperatures using cheap raw materials. The LiFePO$_4$ particles were coated by smaller carbon particles. The sample obtained at 750 °C presents a high initial charge/discharge capacity of 150/133 mAh/g and a capacity retention of 96% after 20 cycles, indicating that the CTR method is effective to synthesize LiFePO$_4$/C cathode material with good electrochemical performance.

References

1. Padhi AK, Nanjundaswamy KS, Goodenough, JB (1997) J Electrochem Soc 144:1188
2. Padhi AK, Nanjundaswamy KS, Masquelier C, Okada S, Goodenough JB (1997) J Electrochem Soc 144:1609
3. Yamada A, Chung SC, Hinokuma K (2001) J Electrochem Soc 148:A224
4. Wu YP, Dai XB, Ma JQ, Chen YJ (2004) Lithium ion batteries: practice and application. Chemical Industry, Beijing
5. Liu H, Li C, Zhang HP, Fu LJ, Wu YP, Wu HQ (2006) J Power Source 159:717
6. Croce F, Epifanio AD, Hassoun J, Deptula A, Olczac T, Scrosati B (2002) Electrochem Solid State Lett 5:A47
7. Wang GX, Yang L, Chen Y, Wang JZ, Bewlay S, Liu HK (2005) Electrochim Acta 50:4649
8. Chung SY, Bloking JT, Chiang YM (2002) Nat Mat 1:123
9. Gouveia DX, Lemos V, Paiva JAC, Souza Filho AG, Mendes Filho J, Lala SM, Montoro LA, Rosolen JM (2005) Phys Rev B 72:24105
10. Liu H, Cao Q, Fu LJ, Li C, Wu YP, Wu HQ (2006) Electrochem Commun 8:1553
11. Huang H, Yin SC, Nazar LF (2001) Electrochem Solid State Lett 4:A170
12. Yang SF, Zavalij PY, Whittingham MS (2001) Electrochem Commun 3:505
13. Yang SF, Song YN, Zavalij PY, Whittingham MS (2002) Electrochem Commun 4:239
14. Croce F, Epifanio AD, Hassoun J, Deptula A, Olczac T, Scrosati B (2002) Electrochem Solid State Lett 5:A47
15. Yang JS, Xu JJ (2004) Electrochem Solid State Lett 7:A515
16. Fu LJ, Liu H, Wu YP, Rahm E, Holze R, Wu HQ (2005) Prog Mater Sci 50:881
17. Bewlay SL, Konstantinov S, Wang GX, Dou SX, Liu HK (2004) Mater Lett 58:1788
18. Sides CR, Croce F, Young VY, Martin CR, Scrosati B (2005) Electrochem Solid State Lett 8:A484
19. Prosini PP, Carewska M, Scaccia S, Wisniewski P, Passerini S, Pasqualib M (2002) J Electrochem Soc 149:A886
20. Zane D, Carewska, b M, Scaccia S, Cardellini S, Prosini PP (2004) Electrochim Acta 49:4259
21. Barker J, Saidi MY, Swoyer JL (2003) Solid State Lett 6:A53
22. Zhu BQ, Li XH, Wang ZX, Guo HJ (2005) Mater Chem Phys 98:373
23. Salah A, Zaghib K, Mauger A, Gendron F, Julien CM (2006) Phys Stat Sol A203:R1
24. Ying JR, Lei M, Jiang CY, Wan CR, He XM, Li JJ, Wang L, Ren JG (2006) J Power Sources 158:543
25. Ravet N, Gauthier M, Zaghib K, Goodenough JB, Mauger A, Gendron F, Julien CM (2007) Chem Mater 19:2595
26. Sato M, Tajimi S, Okawa H, Uematsu K, Toda K (2002) Solid State Ionics 152–153:247
27. Prosini PP, Lisi M, Zane D, Pasquali M (2002) Solid State Ionics 148:45
28. Bard AJ, Faulkner JR (2001) Electrochemical methods, 2nd edn. Wiley, pp 231